Available online at www.sciencedirect.com
ScienceDirect
International Journal of Pharmaceutics 326 (2006) 69–79
INTERNATIONAL JOURNAL OF PHARMACEUTICS
www.elsevier.com/locate/ijpharm

Solid state characterization of olanzapine polymorphs using vibrational spectroscopy

A.P. Ayala [a,b,*], H.W. Siesler [a], R. Boese [c], G.G. Hoffmann [a], G.I. Polla [d], D.R. Vega [d]

[a] *Department of Physical Chemistry, University of Duisburg-Essen, Essen D45117, Germany*
[b] *Departamento de Física, Universidade Federal do Ceará, Caixa Postal 6030, 60.455-900 Fortaleza, CE, Brazil*
[c] *Institut für Anorganische Chemie, Universität Duisburg-Essen, Universitätsstr. 5-7, D-45117 Essen, Germany*
[d] *Unidad de Actividad Física, Comisión Nacional de Energía Atómica, Av. Gral. Paz 1499, 1650 San Martín, Buenos Aires, Argentina*

Received 8 December 2005; received in revised form 28 June 2006; accepted 5 July 2006
Available online 16 July 2006

Abstract

FT-Raman, infrared and near infrared investigations of two polymorphs of olanzapine are presented, establishing the main features that allow the discrimination of these crystalline forms using vibrational spectroscopic methods. *Ab initio* calculations on the basis of the density functional theory were used to determine the stable conformations. The calculated vibrational spectra were compared to the experimental ones in order to identify the conformers corresponding to each polymorph and to assign the vibrational bands to the internal vibrations of the olanzapine molecule. Our results support the hydrogen bonding pattern proposed by the reported crystalline structure and provide valuable information on the structural and thermodynamical relationship between the investigated polymorphs.

Keywords: Olanzapine; Polymorphism; Raman spectroscopy; Infrared spectroscopy; Hydrogen bonding; *Ab initio*; DFT

1. Introduction

Conventional antipsychotics were introduced in the 1950s and all had similar ability to relieve the positive symptoms of schizophrenia. Most of these older "conventional" antipsychotics differed in the side effects they produced. Typical antipsychotics are classified by their chemical structure and the potency with which they bind to dopamine type 2 (D_2) receptors. New antipsychotic agents have shifted from selective dopamine antagonist to compounds that have a broader receptor affinity profile (the so-called *atypical antipsychotics*), characterized by improved clinical efficacy and fewer side effects (Worrel et al., 2000). Compared to the older "conventional" antipsychotics these medications appear to be equally effective for helping reduce the positive symptoms like hallucinations and delusions, but may be better than the older medications at relieving the negative symptoms of the illness, such as withdrawal, thinking problems, and lack of energy.

The first atypical neuroleptic drug was clozapine, followed by olanzapine (Fig. 1), which nowadays is one of the most used drugs of this family. Olanzapine (2-methyl-4-(4-methyl-1-piperazinyl)-10H-thieno-[2,3-*b*] [1,5]benzodiazepine) is a relatively new benzodiazepine which belongs to the class of the thienobenzodiazepines and has proven efficacy against the positive and negative symptoms of schizophrenia, bipolar disorder and other psychosis (Fulton and Goa, 1997; Callaghan et al., 1999; Bhana et al., 2001; Bhana and Perry, 2001; Bitter et al., 2004). Olanzapine is the most widely studied of all first-line atypical agents for the treatment of bipolar disorder and significant evidence of its mood-stabilizing properties exists (Vieta and Goikolea, 2005). Although many atypical antipsychotic drugs have recently been developed and some of them approved for the treatment of schizophrenia, olanzapine is still invaluable for psychosis, having high clinical efficacy (Kelleher et al., 2002; Campiani et al., 2004, 2005).

It was reported that olanzapine crystallizes in at least 25 solid forms, including polymorphs, solvates and hydrates (Capuano et al., 2003; Reutzel-Edens et al., 2003; Wawrzycka-Gorczyca et al., 2004a, b; Polla et al., 2005). The fact that fractions of all three anhydrates could be obtained from desolvation of dif-

* Corresponding author. Tel.: +49 201 1832883; fax: +49 201 1833967.
E-mail address: alejandro.ayala@uni-due.de (A.P. Ayala).

0378-5173/$ – see front matter © 2006 Elsevier B.V. All rights reserved.
doi:10.1016/j.ijpharm.2006.07.023

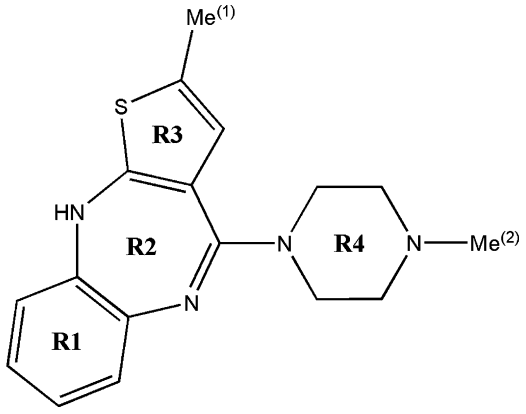

Fig. 1. Molecular structure of olanzapine.

ferent hydrates, or that two of them could convert into a third one through temperature driven processes suggested that a common packing pattern might be present. Thus, the many different structures in which the compound crystallizes probably differ only slightly in their packing arrangement, irrespective of the solvate content. This hypothesis was verified by Polla et al. (2005) and Reutzel-Edens et al. (2003) showing that all of the crystalline forms of olanzapine are built up through the piling of $(olanzapine)_2$ centrosymmetric racemic pairs, stacked into columns parallel to the crystallographic (1 0 0) direction, and connected with each other through N–H···N hydrogen bonds, in the case of polymorph (1), or solvate-mediated interactions (Capuano et al., 2003; Reutzel-Edens et al., 2003; Wawrzycka-Gorczyca et al., 2004a,b; Polla et al., 2005).

Despite the fact that X-ray diffraction is one of the most frequently applied techniques in the study of polymorphism in pharmaceutical compounds, the use of vibrational spectroscopy in this field is gaining increasing attention. Different to X-ray diffraction techniques, which are sensitive to the long-range order, vibrational spectroscopy (infrared (Crupi et al., 2002) and Raman (Fini, 2004)) is primarily sensitive to the short-range structure of molecular solids. Both Raman and infrared spectroscopy provide information on the structure, configuration and conformation in the solid state by probing the vibrations of atoms. Vibrational methods are especially important for the characterization of supramolecular complexes because hydrogen-bonding patterns and other "weak" interactions differ among forms and the functional groups affected display frequency shifts of the vibrational modes. On the other hand, near-infrared (NIR) spectroscopy possesses useful features for use in rapid non-destructive control analyses allowing not only to characterize the different forms of an active principle, but also to determine the polymorphic purity of both the pure product and the final preparation. These characteristic are responsible for the substantial growth in the number of applications of NIR spectroscopy to the identification and quantification of polymorphs of pharmaceutical compounds (Blanco et al., 2000; Fevotte et al., 2004).

In the present work we have focused our interest on the spectroscopic characterization of the two olanzapine anhydrate phases of commercial relevance, viz., those named I and II by Reutzel-Edens et al. (2003), but contradicting the original patents (Bunnell et al., 1996a,b, 1997) which labels them exactly the opposite. In order to avoid confusion, and following the notation used in our previous work (Polla et al., 2005) and the original patent, we call them forms (1) and (2), respectively. The extra anhydrous phase therein reported as form III appeared only as an elusive desolvation product, and was accordingly disregarded from our study. The Raman and infrared (mid and near) spectra of these polymorphs were recorded and analyzed by comparing them with the ones calculated using *ab initio* methods. Thus, the aim of this work is to provide detailed spectroscopic information to characterize the polymorphs of olanzapine, as well as, to shed some light on their structural relationship.

2. Materials and methods

Polycrystalline samples of the anhydrous polymorphic forms (1) and (2) of olanzapine were kindly provided by Gador (Argentine) and Beta (Argentine) laboratories.

Infrared spectra were recorded on a Bruker IFS28 FT-IR spectrometer. KBr pellets of solid samples were prepared from mixtures of 200 mg KBr with 1 mg of sample in a laboratory press. FT-Raman spectra were recorded from the original samples on a Bruker IFS55 FT-IR/FT-Raman spectrometer equipped with a Nd:YAG laser (1064 nm excitation line) and a liquid-nitrogen cooled Ge detector. FT-Raman spectra were acquired by accumulating 1024 scans at a spectral resolution of 2 cm^{-1}. Near infrared spectra were recorded from the original samples with a light-fiber coupled diffuse reflection probe on a Bruker Vector 22 spectrometer.

The electronic structure and optimized geometry of olanzapine were computed within density functional theory using Gaussian 03 (Frisch et al., 2003), employing the hybrid of Becke's non-local three parameter exchange and correlation functional and Lee–Yang–Parr correlation functional (B3LYP) (Lee et al., 1988; Parr and Yang, 1989; Becke, 1993). The 6-31G(d) split valence-shell basis set augmented by d polarization functions on heavy atoms was used (Petersson et al., 1988; Petersson and Allaham, 1991). This basis set provides a good reliable result with acceptable calculation times, especially in the case of the $(olanzapine)_2$ racemic pairs. Full geometry optimizations of a single molecule were carried out without symmetry constraints. In the case of the geometry optimization of the $(olanzapine)_2$ racemic pair, the basis set superposition error (BSSE) was eliminated via the standard counterpoise method of Boys and Bernardi (1970) and Masamura (2001). The optimized structures were compared with experimental results in CHEM3D by superimposing them minimizing the root square distance between selected atoms. The vibrational wavenumbers and absolute Raman scattering and infrared absorption intensities were calculated within the harmonic approximation at the same level of theory used for the optimized geometries. Local minima were verified by establishing that the matrix of energy second derivatives (Hessian) has only positive eigenvalues. The normal coordinate analysis was performed and the potential energy distributions (PED) was calculated among symmetry coordinates for the molecule (Pulay et al., 1979; Fogarasi et al., 1992). For this purpose, a complete set of 120 symmetrized

internal coordinates was defined with help of Pulay's recommendations (Pulay et al., 1979). The vibrational assignments of the normal modes were provided on the basis of the calculated PED by using the program GAR2PED (Martin et al., 1995). Raman and infrared theoretical spectra were calculated using a pure lorentzian band profile (FWHM = 8 cm^{-1}) with our own software. Visualization and checking of calculated data was done by using the CHEMCRAFT program (Zhurko, 2005).

3. Results and discussion

3.1. Geometry optimisation

The crystalline structure of form (1) of olanzapine was determined recently and is characterized by a monoclinic unit cell with four molecules per unit cell, but all of them are related by symmetry operations giving rise to just one independent molecule in it (Reutzel-Edens et al., 2003; Wawrzycka-Gorczyca et al., 2004a,b). These molecules are related by an inversion center forming pairs composed by the two racemic molecules. Fig. 2 shows the crystalline structure of the form (1) of olanzapine, where both enantiomers are included in order to depict the packing of the $(olanzapine)_2$ pairs. Even though no strong intermolecular interactions are associated with these pairs, it is interesting to verify that the $(olanzapine)_2$ pair is the main motif in all of the reported crystal structures of the polymorph and pseudo-polymorphs of olanzapine (Capuano et al., 2003; Reutzel-Edens et al., 2003; Wawrzycka-Gorczyca et al., 2004a,b; Polla et al., 2005). Thus, as starting point of our quantum mechanical calculations, a single olanzapine molecule was calculated and its geometry compared with the one obtained from the crystalline structure. This geometry optimization produced a molecule which is remarkably similar to the one of the crystallographic asymmetric unit. By superimposing both molecules using a least squares algorithm and minimizing the distances among the non-hydrogen atoms, we obtained an average atomic deviation as small as 0.098 Å. Similar results were obtained by calculating the $(olanzapine)_2$ pair. As the centrosymmetric pair is a common entity among the solid forms of olanzapine, the geometry optimization of the pair was constrained to remain in the C_i point group. The optimitzed pair is stable and characterized by a binding energy of 6.32 kJ/mol. By superimposing the enantiomers to the determined crystalline structure independently, the average atomic deviation is slightly reduced to 0.087 Å compared to the single molecule calculation. According to Reutzel-Edens et al. (2003), no specific intermolecular interactions stabilize the racemic pairs, which are packed due to the spatial complementarity of the opposite enatiomers (electrostatic interaction). Conversely, Wawrzycka-Gorczyca et al. (2004a,b) associated the pairs stability with three types of multiple C–H···π contacts. Independently of the character of the intermolecular interaction, the packing may be described by the distance between the centroids of the phenyl and piperazynil rings. The main difference between the experimental and calculated pairs geometries is the expansion of the intermolecular distance from 4.665 to 5.120 Å. The origin of this expansion of the racemic pair may be understood by comparing the corresponding intermolecular distance among the reported structures of the olanzapine polymorphs and pseudo-polymorphs. Thus, it can be observed that the shortest distance corresponds to the crystalline form of the pure compound, where the racemic pairs are in a close packed arrangement having a six-fold coordination (Fig. 2a). On the other hand, in the pseudo-polymorphs the extra molecules are placed among the racemic pairs distorting its close packing, as it can be observed in the case of the dihydrate showed in Fig. 2b, and allowing the increasing of the intermolecular distance. Thus, the pseudo-polymorphs exhibit higher intermolecular distances around 4.8 Å suggesting that quantum mechanical calculation provides an upper limit for the $(olanzapine)_2$ conformation.

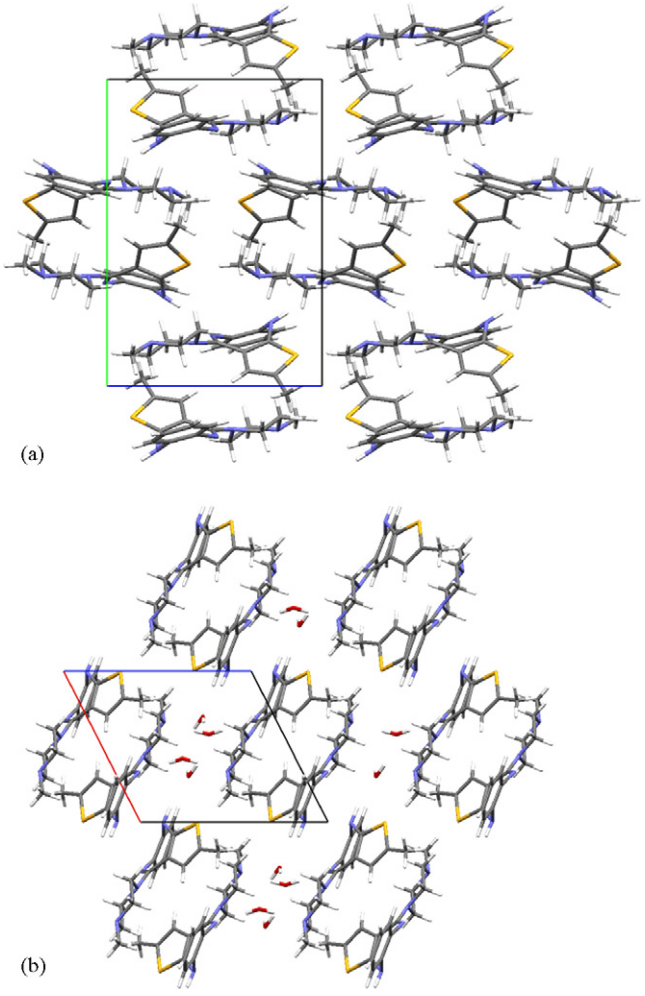

Fig. 2. Crystalline structure of: (a) form (1) and (b) dihydrate of olanzapine. Extra molecules are presented to depict the packing of the $(olanzapine)_2$ pairs.

The geometry optimization results show that the crystalline field induces almost no conformational changes in the most stable structure of olanzapine (form (1)). However, a conformational search for energetic minima was performed by Reutzel-Edens et al. (2003), and these authors found two non-equivalent olanzapine conformers, namely A and B (Fig. 2). Both conformers exhibit approximately the same thiophene-benzodiazepine geometrical configuration but in conformer A the piperazinyl ring is in the typical chair conformation and is almost parallel to

the aromatic ring while, in conformer B, these rings are almost perpendicular with the piperazinyl ring in a twisted boat conformation (see Fig. 2). Despite the conformational differences, the energies of the two conformers are very close with conformer B being 28.27 kJ/mol less stable than conformer A. This value is slightly higher than the one reported by Reutzel-Edens et al., but the small discrepancy may be associated with differences in the calculation methods used by us and the previously published works. However, in both cases the energy difference between the two conformers is small enough to allow a conformational change based on the effect of different crystalline environments. Since there is no crystal structure reported for form (2), which is monotropically related to form (1) and apparently has also one independent molecule per unit cell, the possibility that this transformation is associated with a conformational change should be considered. We will discuss this issue later on the basis of the vibrational spectra of the investigated crystalline forms of olanzapine.

3.2. Vibrational spectra

The Raman and infrared spectra of the forms (1) and (2) of olanzapine, recorded at room temperature, are presented in Figs. 3 and 4. According to the crystal structure of form (1), there are four olanzapine molecules in the unit cell, pairwise related by an inversion center. As a consequence, the olanzapine recemic mixture forming the previously discussed pairs cannot be distinguished by vibrational spectroscopy. Since all atoms occupy general sites with multiplicity 4, the vibrational modes are equally distributed among the irreducible representations of the $P2_1/c$ space group. Thus, for each of the irreducible representations, 120 modes corresponding to the internal vibrations of olanzapine are expected, being distributed, due to the inversion center and according to the mutual exclusion principle, in two Raman active (A_g and B_g representations) and two infrared active (A_u and B_u representations) bands. In addition, librational ($3A_u + 3B_u + 3A_g + 3B_g$) and lattice ($2A_u + 1B_u + 3A_g + 3B_g$) modes are predicted by the factor group analysis to be observed in the low wavenumber spectral region.

Since the geometry-optimized molecule resulting form the DFT calculation reproduced very well the one of the crystalline structure of form (1), let us first discuss the vibrational spectrum of this polymorph in terms of the normal modes analysis of the olanzapine molecule. A list of selected observed Raman and infrared bands of form (1) are presented in Table 1. In general, it may be noticed that the energies of the Raman and infrared bands are very close and, as it will be shown later, no A_u/B_u (A_g/B_g) split is observed, suggesting that the crystalline field is not strong enough to split the internal modes of olanzapine. Table 1 also includes the PED distribution calculated from the optimized structure of conformer A, where the contributions are organized according to the main molecular groups of olanzapine (labeled as in Fig. 1) neglecting group contributions lower than 10%. The normal modes associated to the benzene moiety (RA) are best described in terms of the Wilson's notation (Varsanyi, 1969), since these vibrational modes are recognizable by showing group characteristic frequencies or systematic behaviors.

Starting from high wavenumbers, the first feature observed in the vibrational spectra is the stretching vibration of the only NH bond present in the molecule. This band is intense in the infrared spectra but shows only low intensity in the Raman one. The broad band shape and the shift toward lower wavenumbers, pointed out the involvement of this band in hydrogen bonds in excellent agreement with the reported crystalline structure (Reutzel-Edens et al., 2003; Wawrzycka-Gorczyca et al., 2004a,b). At lower wavenumbers, the bands associated with the CH stretching are observed. The PED calculations suggest that the first group corresponds to the CH stretching of the thiophene and benzene rings, whereas the remaining bands are the symmetric and antisymmetric modes of the two methyl groups and the methylene functionalities of the piperazine ring. It is interesting to notice that more bands are observed in this region than expected by considering the molecular structure; however the extra bands may be associated with overtones and combinations of lower energy modes.

Proceeding to lower energy, the region between 1600 and 1500 cm^{-1} is dominated by the bands associated with the double bonds, which are partially coupled to CH and NH bending deformations. These bonds may be classified in three groups: the C=C ones belonging to the benzene and thiophene rings and the C=N bond of the azepine ring. C=C bonds (*8a* and *8b*) are expected to be weak in infrared but strong in Raman, as it is verified in the case of the 1516 cm^{-1} band, whereas the C=N should exhibit the opposite behavior. The DFT calculation suggests that the highest energy band is associated with the C=N bond but this can not be confirmed by the experimental results

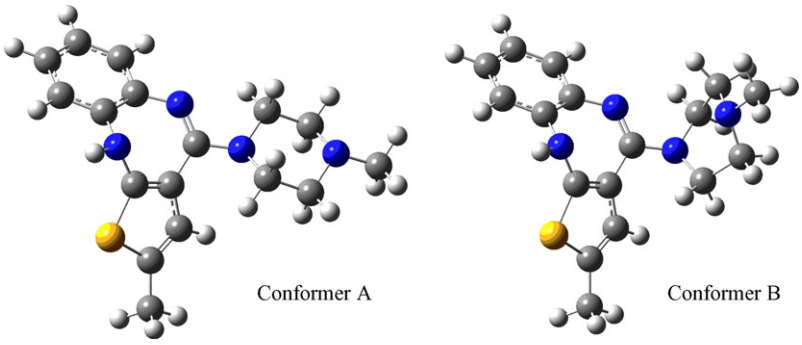

Fig. 3. Olanzapine conformers obtained from DFT geometrical optimizations.

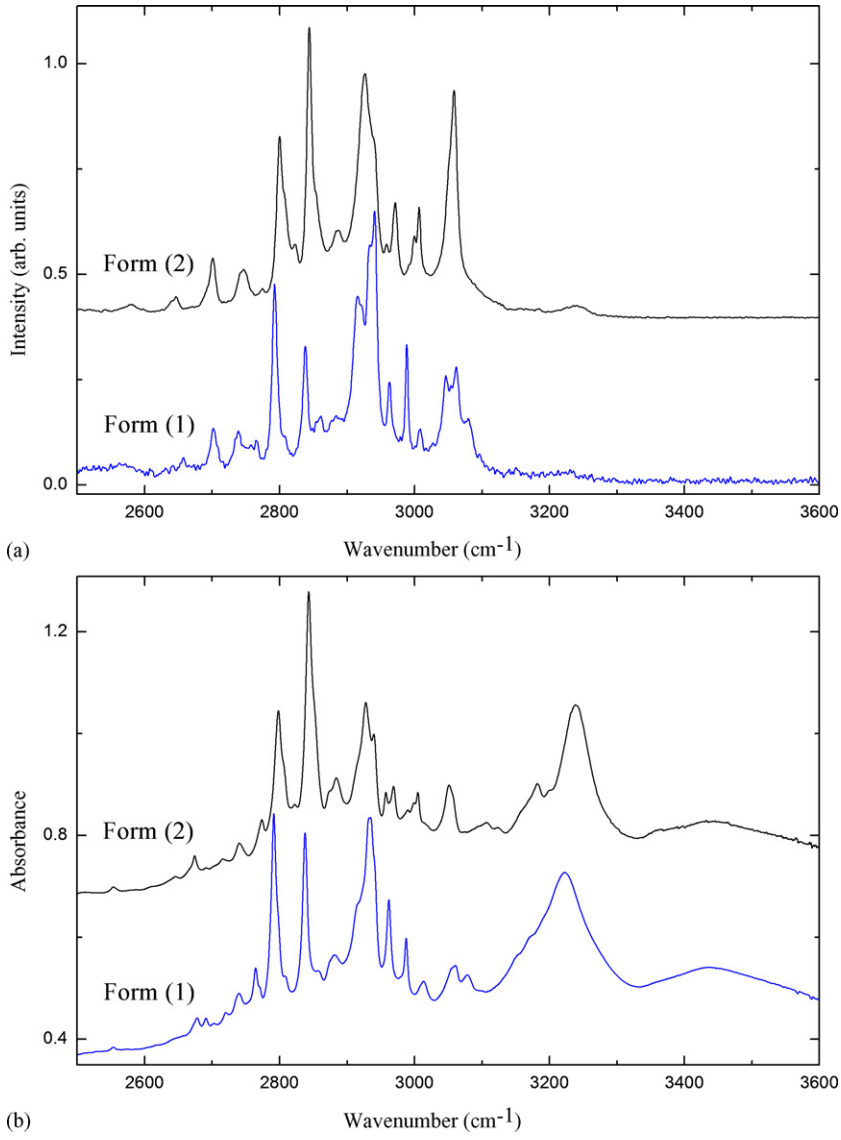

Fig. 4. (a) Raman and (b) infrared spectra of the polymorphs of olanzapine above 2500 cm^{-1}.

since the strongest IR band in this region seems to correspond to the band at 1584 cm^{-1} (Fig. 4b, form (1)). Independently of the possible differences between theoretical and experimental data, the fact that the C=N band is observed below 1600 cm^{-1} evidences the participation of this bond in the hydrogen bond pattern of the form (1) of olanzapine, as it was proposed by the X-ray diffraction structure refinement (Reutzel-Edens et al., 2003; Wawrzycka-Gorczyca et al., 2004a,b).

The next spectral region (1500–1300 cm^{-1}) is mainly dominated by the deformations of the methyl, methylene and C–H groups. However, these bands are highly overlapped and it is difficult to perform an accurate assignment. The PED distribution of these vibrations shows that they are partially localized and some of them exhibit a pure character (e.g. $\delta(Me^{(1)})$ at 1411 cm^{-1}), whereas, in the case of coupling, it is usually between neighboring groups (e.g. methylene deformation of the piperazinyl group coupled to the methyl $Me^{(2)}$ at 1470 cm^{-1}). Between 1300 and 1100 cm^{-1}, the contribution of the C–C and C–N stretching is dominant and the vibrational modes are spread over the complete molecule having contributions of different moieties, as may be observed in Table 1. Below 1100 cm^{-1}, vibrational modes recover some localization and the corresponding bands are less overlapped. In this region, some relevant features are identified, such as the Raman band at 1043 cm^{-1}, characteristic of the in plane breathing deformation of the benzene (1), and the infrared band at 745 cm^{-1}, associated with the out of plane deformation of the CH bonds of the same group (11). The deformations of the piperazinyl group, coupled to $Me^{(2)}$ (1009 cm^{-1}) or to the azepine and thiophene moieties (965 cm^{-1}), are well identified in the infrared spectra. At lower wavenumbers, the main components of the vibrational modes are the deformation and torsions of the rings giving rise to highly coupled movements. Finally, the low energy vibrational modes originate from the deformations of the skeleton of the molecule and the lattice vibrations. As it will be shown later, these vibrational modes are highly sensible to the crystalline form and

Table 1
Observed Raman and infrared bands of the polymorphs of olanzapine (forms (1) and (2))

Form (1)		Form (2)		PED
Raman	IR	Raman	IR	
1594	1593	1600	1601	**R1**[*8a*](24) + **R2**[ν(CN)](63)
	1584	1586	1589	**R1**[*8a*](51) + **R2**[ν(CN) + δ(NH)](17) + **R3**[ν(CC)](17)
1577		1580	1582	**R1**[*8b*](82)
1558	1558	1559	1559	**R1**[*8b*](23) + **R2**[ν(CN)](15) + **R3**[ν(CC) + δ(CH)](53)
1517	1516	1522	1523	**R2**[δ(NH)](12) + **R3**[ν(CC)](62) + **Me**$^{(1)}$[δ(CH$_3$)](10)
1499		1509	1508	**R1**[*19b*](67) + **R2**[δ(NH)](23)
1472	1470		1469	**R4**[δ(CH$_2$)](15) + **Me**$^{(2)}$[δ(CH$_3$)](83)
1467		1467		**R4**[δ(CH$_2$)](73) + **Me**$^{(2)}$[δ(CH$_3$)](25)
1461	1460	1461		**R4**[δ(CH$_2$)](91)
1454			1455	**Me**$^{(1)}$[δ(CH$_3$)](87)
1445	1448		1443	**R4**[δ(CH$_2$)](91)
1440		1440		**R1**[*19a*](15) + **Me**$^{(1)}$[δ(CH$_3$)](69)
1435	1435			**R1**[*19a*](48) + **R2**[δ(NH)](26) + **Me**$^{(1)}$[δ(CH$_3$)](17)
1419	1420	1423	1426	**R4**[δ(CH$_2$)](18) + **Me**$^{(2)}$[δ(CH$_3$)](79)
1411	1412	1417	1418	**Me**$^{(1)}$[δ(CH$_3$)](89)
1382		1382	1381	**R1**[*19a*](43) + **R2**[δ(NH)](36)
1377	1379			**R4**[ω(CH$_2$)](78) + Me$^{(2)}$[δ(CH$_3$)](13)
1370	1369	1366	1365	**R2**[ν(CC) + δ(NH)](23) + **R4**[ω(CH$_2$)](30) + ν(C[**R2**]N[**R4**])](31)
	1358	1357	1357	**R4**[ω(CH$_2$)](83)
1353	1352			**R4**[ω(CH$_2$)](88)
1341	1341	1343	1345	**R3**[ν(CC) + δ(CH)](59) + **R4**[ω(CH$_2$)](18)
1331	1331	1330		**R4**[ω(CH$_2$)](88)
1294	1294	1294	1297	**R1**[*14*](17) + **R4**[γ(CH$_2$)](70)
1290	1289	1288	1290	**R1**[*14*](76) + **R4**[γ(CH$_2$)](10)
1281	1282		1284	**R1**[*14*](10) + **R4**[γ(CH$_2$)](68) + **Me**$^{(2)}$[δ(CH$_3$)](13)
	1271	1269	1269	**R1**[*3*](36) + **R2**[ν(CN)](16) + **R4**[ν(CN)](27)
1259	1259	1260	1261	**R1**[*3*](18) + **R2**[ν_{ring}](29) + **R4**[γ(CH$_2$)](32)
1248	1247	1251	1253	**R1**[*3*](35) + **R2**[δ(NH) + ν(CN)](17) + **R4**[ν(CN) + γ(CH$_2$)](28)
1224	1223	1221	1221	**R1**[*18b*](12) + **R2**[ν_{ring}](21) + **R4**[ν(CN) + γ(CH$_2$)](37)
	1215			**R1**[*18b*](27) + **R2**[ν_{ring}](39) + **R4**[γ(CH$_2$)](16)
1202	1201	1202	1198	**R4**[γ(CH$_2$)](98)
		1190	1190	**R2**[ν(CN)](26) + **R3**[δ(CH) + ν(CC)](43)
1179	1179	1179	1179	**R1**[*18b*](11) + **R2**[*def.*](17) + **R3**[δ(CH) + ν(CC)](27) + **R4**[γ(CH$_2$)](19) + **Me**$^{(1)}$[δ(CH$_3$)](11)
				R1[*9a*](97)
1154	1155	1157	1157	**R4**[ν_{ring} + γ(CH$_2$)](53) + **Me**$^{(2)}$[ν(CN) + ρ(CH$_3$)](30)
	1152	1150	1150	**R4**[ν_{ring} + γ(CH$_2$)](58) + **Me**$^{(2)}$[ν(CN) + ρ(CH$_3$)](36)
1142	1143		1142	**R4**[ν_{ring} + γ(CH$_2$)](26) + **Me**$^{(2)}$[ν(CN) + ρ(CH$_3$)](34)
	1120		1120	**R1**[*18a*](20) + **R3**[δ_{ring} + δ(CH)](32) + **Me**$^{(1)}$[ν(CC) + ρ(CH$_3$)](30)
1103	1102	1105	1105	**R1**[*18a*](54) + **R2**[ν(CN)](13) + **R3**[δ(CH)](13)
	1083		1080	**R4**[ν_{ring} + γ(CH$_2$)](65) + **Me**$^{(2)}$[ρ(CH3)](27)
	1073	1072	1071	**R4**[ν_{ring} + γ(CH$_2$)](76) + **Me**$^{(2)}$[ρ(CH3)](17)
1051	1050	1051	1051	**R4**[ν_{ring} + γ(CH$_2$)](72) + **Me**$^{(2)}$[ρ(CH3)](23)
			1046	**Me**$^{(1)}$[ρ(CH$_3$)](87)
1043	1042	1043	1043	**R1**[*1*](79)
				R2[δ_{ring}](14) + **R4**[δ_{ring} + γ(CH2)](72)
	1009	1004	1005	**R4**[δ_{ring}](96)
		986		**R3**[δ_{ring}](24) + **Me**$^{(1)}$[ρ(CH$_3$) + ν(CC)](70)
965	965	973	971	**R2**[δ_{ring}](15) + **R3**[ν(CS)](10) + **R4**[δ_{ring}](51)
	941	941		**R1**[*5*](99)
	934		935	**R4**[δ_{ring} + ρ(CH$_2$)](78) + **Me**$^{(2)}$[ρ(CH3)](12)
	927		930	**R1**[*17b*](97)
886	887	902	904	**R1**[*12*](48) + **R2**[δ_{ring}](38)
	858	862	855	**R3**[o(CH)](62) + **R4**[ρ(CH$_2$)](27)
852	853	851	851	**R1**[*17a*](50) + **R3**[o(CH)](17) + **R4**[ρ(CH$_2$)](23)
845	845	844	844	**R1**[*17a*](45) + **R3**[o(CH)](23) + **R4**[ρ(CH$_2$)](20)
819	817	816	817	**R2**[δ_{ring}](29) + **R3**[δ_{ring}](28) + **R4**[ν(CN)](15)
	813		832	**R1**[*6b*](16) + **R2**[δ_{ring} + o(NH)](27) + **R3**[ν(CS)](26) + **R4**[ν(CN)](22)
784	783	786	787	**R2**[δ_{ring}](10) + **R4**[δ_{ring} + ρ(CH$_2$)](67)
769	767	777	777	**R1**[*11*](24) + **R2**[δ_{ring}](29) + **R4**[δ_{ring}](24)
748	745	761	757	**R1**[*11*](79)

Proposed assignment and potential energy distribution (PED) for vibrational normal modes. Types of vibration: ν, stretching; δ, deformation; ◯, out-of-plane bending; ω, wagging; γ, twisting; ρ, rocking. The benzene moiety modes are labeled following the Wilson's notation (Varsanyi, 1969).

provide a good tool to discriminate the polymorphs of olanzapine.

Having assigned the most important features of the Raman and infrared spectra of the form (1), we are able to compare the corresponding spectra of the crystalline forms of olanzapine in order to provide a spectroscopic methodology to differentiate them and to give some insight into the crystalline structure of form (2). In Figs. 3 and 4 we compared the infrared and Raman spectra of forms (1) and (2) of olanzapine, whereas in Table 1, the wavenumber positions of the corresponding bands are listed. By comparing the C–H and N–H stretching region, it is possible to verify shifts of several bands (Fig. 3) indicating qualitative changes that may fingerprint the crystalline forms. One of the most interesting changes is associated with the NH stretching band, which shifts 19 cm^{-1} toward higher wavenumbers and is reduced in half-band width from 83 (Form (1)) to 53 cm^{-1} (Form (1)). The lowering of the linewidth in form (2) reveals subtle bands of the infrared spectrum between 3100 and 3200 cm^{-1} which have been superimposed by the ν(NH) band in form (1). However, these bands seem not to be associated with fundamental vibrations but having their origin in overtones of the double bond stretching bands, as for example: 3180 $cm^{-1} = 2 \times \nu$(C=C) (1589 cm^{-1}). It is well known that the stronger the hydrogen bond, the lower the NH stretching wavenumber and the wider the infrared band. On the other hand, the reported crystalline structure and the analysis of the vibrational spectra of form (1) support the existence of a NH···N hydrogen bond, being the primary intermolecular interaction of this structure. The ν(NH) absorption band of the form (2) lying at higher wavenumbers as that of form (1) evidences a larger entropy for form (2) than form (1). The latter is, related to the free-energy curves, form (1) is the thermodynamic stable form at 0 K. This is consistent with the infrared rule (Burger and Ramberger, 1979a,b; Grunenberg et al., 1996) and provides further support to the monotropic relationship between forms (1) and (2) previously reported (Reutzel-Edens et al., 2003; Polla et al., 2005).

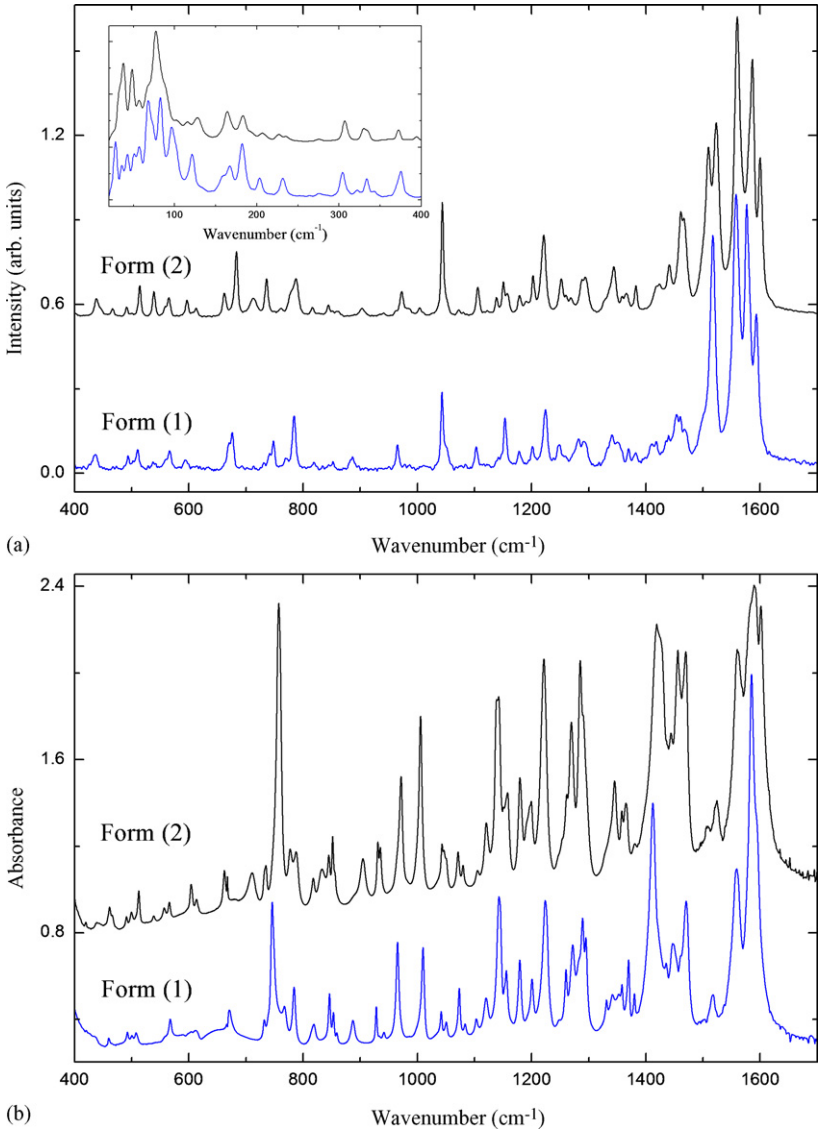

Fig. 5. (a) Raman and (b) infrared spectra of the polymorphs of olanzapine below 1700 cm^{-1}.

The most remarkable differences between the vibrational spectra of forms (1) and (2) of olanzapine can be observed in the region of the stretching vibrations of the double bonds, which is expanded in Fig. 5. Thus, form (2) is characterized by the splitting of the Raman band at 1517 cm^{-1} in form (1) and the appearance of a new infrared band at 1601 cm^{-1}. Recalling that the single crystal structure establishes that just one independent olanzapine molecule is present in the unit cell, this splitting might be attributed to the existence of at least two independent molecules in form (2). However, this hypothesis can be ruled out because it is not throughout the whole spectrum and just few bands exhibit such a splitting; moreover solid state NMR results also suggest that all of the polymorphs of olanzapine are characterized by just one independent molecule per unit cell (Reutzel-Edens et al., 2003).

Another effect that should be considered is the possibility of a conformational change. Quantum mechanical calculations show that two olanzapine conformers (Fig. 2) exhibit very similar energies and a transformation between them could be induced by the crystalline field (Reutzel-Edens et al., 2003). In order to verify this argument, the Raman and infrared spectra of both conformers were calculated using DFT and plotted, in Fig. 5. The vibrational frequencies obtained from the DFT calculations were scaled by 0.962 in order to reproduce the experimental frequencies as close as possible. First, one may notice the good agreement between the calculated spectrum of conformer A and the experimental spectrum of form (1), confirming the previously discussed similarity between the free molecule and the one in form (1). Furthermore, Fig. 5 clearly shows that the splitting of the 1517 cm^{-1} Raman band, also observed in the infrared spectrum, cannot arise from conformer B. The comparison of the conformers endorse this assumption, since the main changes between conformers A and B are associated with the piperazinyl ring, which does not exhibit any double bond. The only effect of the conformational change in this spectral region is associated with the band at about 1600 cm^{-1} in the calculated spectra. As stated previously, this band corresponds to the C–N stretching which, due to the absence of hydrogen bonds in the calculation, appears at higher energy. Since the carbon atom of this bond is also linked to the piperazinyl ring trough a C–N bond, conformational changes in this ring may be reflected in the double bond giving rise to the shift observed in Fig. 5.

The previous discussion suggests that neither conformational changes nor the increase in the number of independent molecules per unit cell are responsible for the changes in the vibrational spectra of the olanzapine polymorphs. However, the analysis of the NH band supports the weakening of the hydrogen bonding in form (2). Based on this assumption, the appearance of a new band in the infrared spectrum (Fig. 5b) could be associated with the shift toward higher energies of the C=N stretching, which is directly involved in the hydrogen bond. Due to the effect of the intermolecular interactions, it is difficult to assign the bands located between 1530 and 1630 cm^{-1} in form (1) to the calculated vibrational spectra, as it was verified in the case of the ν(C=N). On the other hand, the band at 1517 cm^{-1} (form (1)) is very well resolved in both experimental and calculated spectra. The PED analysis shows that this band corresponds to the coupling of the δ(NH) with the ν(C=C) of the thiophene ring and the deformation of the methyl group linked to it (see Fig. 6 and Table 1). Apart from this band, in the Raman spectra of form (1), a very weak band at 1499 cm^{-1} may be identified, which could also be associated with the δ(NH), but, in this case, coupled with the δ(CH) of the benzene ring (see Fig. 6 and Table 1).

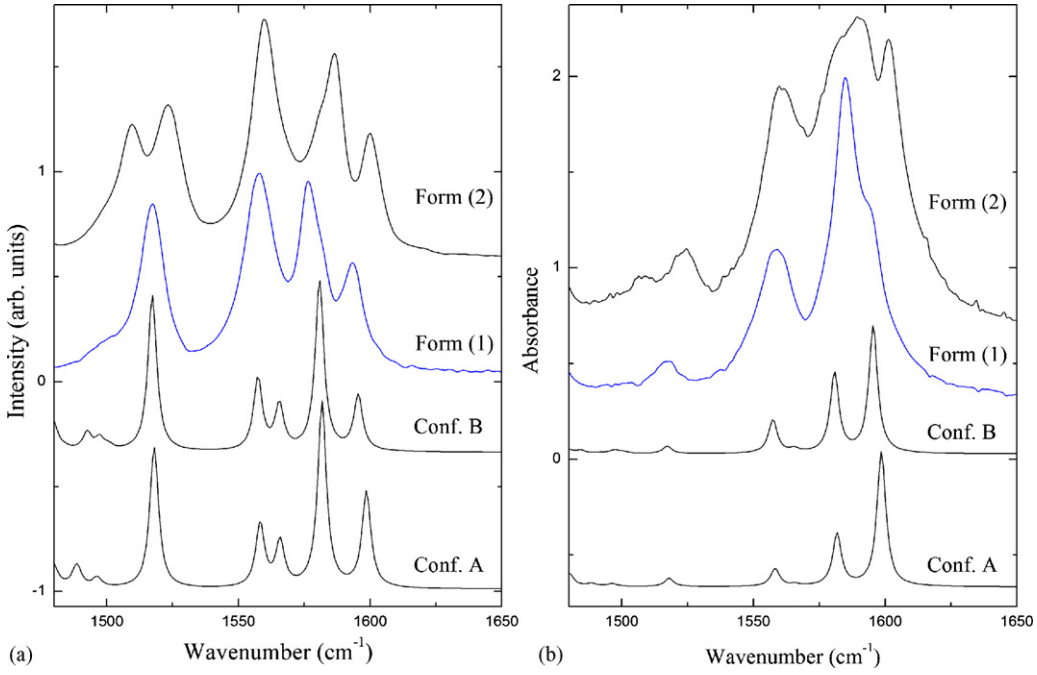

Fig. 6. Comparison of: (a) Raman and (b) infrared spectra of the polymorphs of olanzapine in the ν(C=C) and ν(C=N) double bond region with the calculated spectra of conformers A and B.

The contribution of the δ(NH) deformation to these bands should make them sensitive to modification in the N···HN interaction. As a consequence, the weaker hydrogen bond of form (2) could induce apparent splitting of the 1517 cm^{-1} band by increasing its energy, as well as the one of the 1499 cm^{-1} band, according to the assignment proposed in Fig. 6. This kind of behavior of the δ(NH) may be classified as anomalous, since it is expected that for weaker hydrogen bonds this band should decrease in energy. However, other bands associated with deformations of the NH bond also move to higher wavenumbers in form (2). This is the case of the very broad band around 650 cm^{-1} (IR), associated with an out of plane NH deformation, which moves to 710 cm^{-1} and strongly reduces its linewidth. Notice that the weakening of the hydrogen bonds by augmenting only the N···HN distance not necessarily gives rise to a new polymorph, as it is observed in the case of the thermal expansion of a crystal. On the other hand, one may expect that a structural transformation should be accompanied not only by changes in the distance between the molecules but also their relative orientations. In such a case, the "normal" behavior of the δ(NH) when the hydrogen bond becomes weaker will compete with the changes in the N···HN angle and should originate the anomalous effect observed in olanzapine.

By comparing the rest of the vibrational spectra of forms (1) and (2) with the help of the PED distribution of Table 1, one may notice that the bands which fingerprint the different forms are closely related to the azepine ring and the vibration of "external" atoms. Thus XH deformations exhibit the most evident changes from one polymorph to the other. As an example one may cite the region around 1400 cm^{-1} and the out of plane bending of the benzene moiety (748 cm^{-1} in form (1)). On the other hand, bands associated with deformation of the "internal" structure are less sensitive to changes of the crystalline form, as it may be verified in the case of the ν(C=C) at 1558 cm^{-1} or the deformation of the benzene and piperazinyl group around 1043 and 970 cm^{-1}, respectively. These observations also agree with the hypothesis that the crystalline forms are related by rearrangements of the $(olanzapine)_2$ racemic pairs more than conformational changes. In this way, the atoms at the rim of the molecule are more sensitive to the changes of the environment than those atoms supporting the molecular skeleton, which remains almost unaltered.

The Raman spectra of the two olanzapine polymorphs below 400 cm^{-1} are shown in the insert of Fig. 3a. This spectral region is characterized by deformations of the molecular skeleton and, at very low energies, the lattice vibrations and molecular librations (<100 cm^{-1}). By comparing these spectra one may notice that, above 100 cm^{-1}, where the skeletal deformations dominate, there are few qualitative changes between the Raman bands of forms (1) and (2), showing that the two crystalline forms do not exhibit important conformational differences among the corresponding olanzapine molecules. On the other hand, lattice and librational modes are highly sensitive to the polymorph since they directly reveal changes in the fundamental translational rules, which determine the crystalline structure.

Finally, Fig. 7 shows the near infrared spectra of the two polymorphs of olanzapine investigated in this work. This technique has been demonstrated to be a very useful tool to investigate polymorphism in pharmaceutical compounds because NIR spectra can be acquired without preparation from the original samples, and especially due to the ability of providing quantitative results when combined with chemometric calibration methods. However, since the NIR spectrum is dominated by overlapping overtones and combinations of the fundamental vibrations of the molecule, its interpretation in terms of a detailed assignment of the observed bands is very difficult. However, the crystalline character of the investigated compounds gives rise to narrow bands which allow us to perform a qualitative analysis of the spectra. Several features below 5200 cm^{-1} are distinctive of each sample allowing the identification of the crystalline form by direct inspection of the NIR spectra (Fig. 7a). In this region one may identify two groups of bands: the ones below 4400 cm^{-1}, which are associated with ν(CH) + δ(CH) combination bands, and those between 4400 and 4900 cm^{-1}, corresponding to ν(CH) + ν(C = X) and ν(NH) + δ(NH) combination bands. In the region above 5000 cm^{-1} (Fig. 7b), the first overtones (5500–6500 cm^{-1}) and second overtones (8300–9000 cm^{-1}) of the CH and – with much lower intensity – NH stretching vibrations, as well as the combinations 2 ν(CH) + δ(CH) (−7000 cm^{-1}), may be identified (Fig. 8).

As in the case of the fundamental vibrations, the hydrogen bonding also influences the behavior of the NIR bands. Thus, XH vibrational modes associated with this kind of interaction become more harmonic and, as a consequence, their NIR activ-

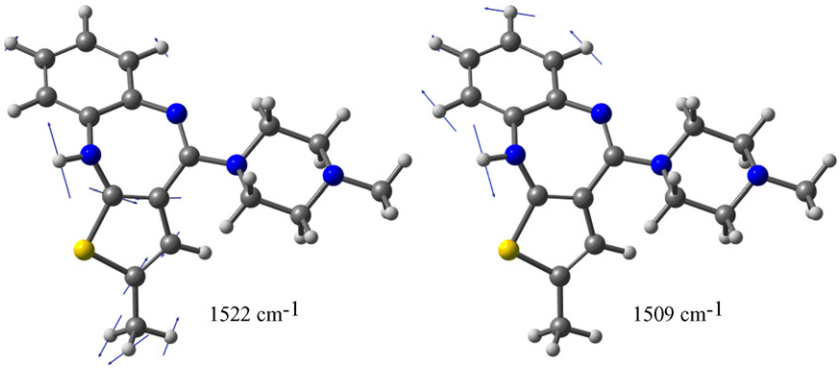

Fig. 7. Displacement vectors of the proposed assignment of some vibrational modes of form (2).

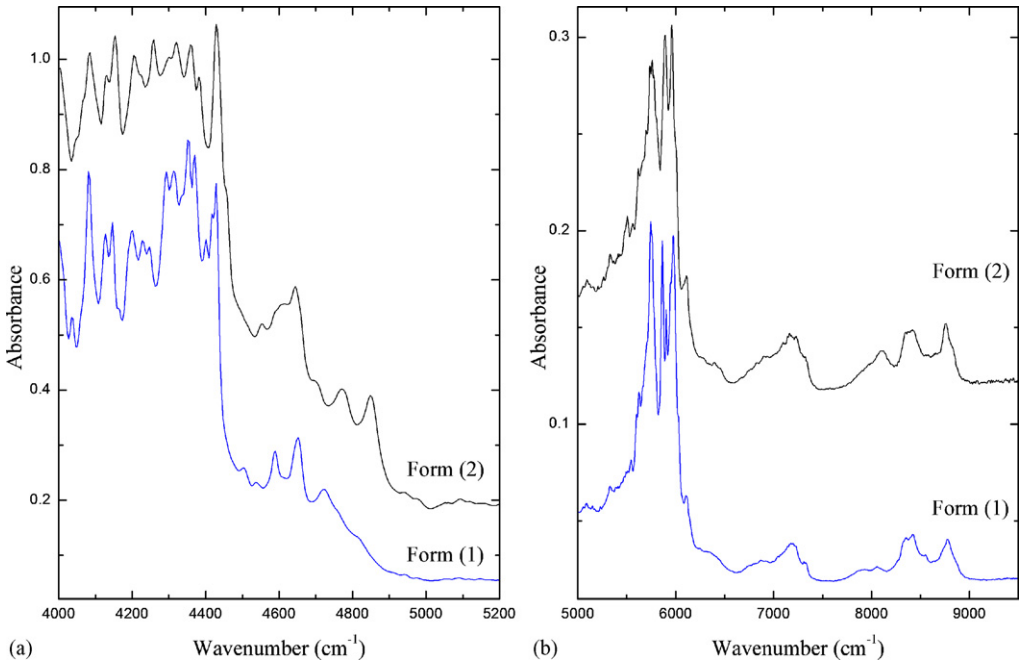

Fig. 8. Near infrared spectra of the polymorphs of olanzapine.

ity is strongly reduced. Olanzapine is a good example of this effect, since, for example, the CH stretching modes, which are not hydrogen-bonded, exhibit very sharp bands, as combinations with δ(CH) ($-4200\,cm^{-1}$) or as overtones (-5700 and $-8500\,cm^{-1}$). Conversely, the strong NH$\cdots$N hydrogen-bond leads to the almost complete disappearance of the first overtone of the ν(NH) band, observed as a weak and wide shoulder around $6300\,cm^{-1}$. The weakening of the hydrogen bond in form (2) has lead to a slight shift of the ν(NH) fundamental toward high wavenumbers accompanied by a small reduction of the linewidth of this band. In the near-infrared region, this effect may be associated with the changes observed in the ν(NH) + δ(NH) combinations bands ($-4750\,cm^{-1}$).

4. Conclusions

Vibrational spectroscopy and density functional calculation have been applied to the investigation of the two olanzapine anhydrate phases of commercial relevance. Geometrical optimizations show that the most stable conformer is the one exhibited by the crystalline structure of form (1). By combining experimental Raman and infrared spectroscopic data with calculated vibrational spectra, most of the bands of this polymorph could be assigned to the fundamental vibrations of the molecule. The vibrational spectrum of form (1) exhibits features characteristic of a hydrogen bonded molecule, confirming the intermolecular interactions as manifested by the known crystal structure. The comparison of the experimental and calculated results ruled out the possibility that the forms (1) and (2) are related by a conformational change. Most of the changes identified in the vibrational spectra of form (2) are associated with atoms involved directly or indirectly to the NH–hydrogen bond. Thus our results suggest that a weakening of the intermolecular interaction gives rise to a lower density of form (2) and providing additional support to the monotropic relationship proposed for the olanzapine forms.

Acknowledgements

A.P. Ayala acknowledges financial support from the Brazilian Agency CNPq (PDE, Proc. 201246/2004-0), the Universidade Federal do Ceará and UNESCO (IBSP Proj. 3-Br-05).

References

Becke, A.D., 1993. Density-functional thermochemistry. 3. The role of exact exchange. J. Chem. Phys. 98, 5648–5652.

Bhana, N., Foster, R.H., Olney, R., Plosker, G.L., 2001. Olanzapine—an updated review of its use in the management of schizophrenia. Drugs 61, 111–161.

Bhana, N., Perry, C.M., 2001. Olanzapine—a review of its use in the treatment of bipolar I disorder. CNS Drugs 15, 871–904.

Bitter, I., Dossenbach, M.R.K., Brook, S., Feldman, P.D., Metcalfe, S., Gagiano, C.A., Furedi, J., Bartko, G., Janka, Z., Banki, C.M., Kovacs, G., Breier, A., 2004. Olanzapine versus clozapine in treatment-resistant or treatment-intolerant schizophrenia. Prog. Neuro-Psychopharmacol. Biol. Psychiatry 28, 173–180.

Blanco, M., Coello, J., Iturriaga, H., Maspoch, S., Perez-Maseda, C., 2000. Determination of polymorphic purity by near infrared spectrometry. Anal. Chim. Acta 407, 247–254.

Boys, S.F., Bernardi, F., 1970. Calculation of small molecular interactions by differences of separate total energies—some procedures with reduced errors. Mol. Phys. 19, 553.

Bunnell, C.A., Hendriksen, B.A., Larsen, S.D., 1996a. Crystal Forms of a Thieno (2,3-*b*) (1,5)Benzodiazepine Derivative and Process for their Preparation. Eli Lilly and Company, USA and Lilly Industries Ltd., England (EP Patent No. 733635).

Bunnell, C.A., Hendriksen, B.A., Larsen, S.D., 1996b. Process and Crystal Forms of 2-Methyl-thieno-benzodiazepine. Eli Lilly and Company, USA and Lilly Industries Ltd., England (WO Patent No. 9630375).

Bunnell, C.A., Hotten, T.M., Larsen, S.D., Tupper, D.E., 1997. Process and Solvate of 2-Methyl-thieno-benzodiazepine. Eli Lilly and Company, USA and Lilly Industries Ltd., England (US Patent No. 5631250).

Burger, A., Ramberger, R., 1979a. On the polymorphism of pharmaceuticals and other molecular crystals. I. Theory of thermodynamic rules. Mikrochim. Acta II, 259–271.

Burger, A., Ramberger, R., 1979b. On the polymorphism of pharmaceuticals and other molecular crystals. II. Applicability of thermodynamic rules. Mikrochim. Acta II, 273–316.

Callaghan, J.T., Bergstrom, R.F., Ptak, L.R., Beasley, C.M., 1999. Olanzapine—pharmacokinetic and pharmacodynamic profile. Clin. Pharmacokinet. 37, 177–193.

Campiani, G., Butini, S., Fattorusso, C., Catalanotti, B., Gemma, S., Nacci, V., Morelli, E., Cagnotto, A., Mereghetti, I., Mennini, T., Carli, M., Minetti, P., Di Cesare, M.A., Mastroianni, D., Scafetta, N., Galletti, B., Stasi, M.A., Castorina, M., Pacifici, L., Vertechy, M., Di Serio, S., Ghirardi, O., Tinti, O., Carminati, P., 2004. Pyrrolo [1,3]benzothiazepine-based serotonin and dopamine receptor antagonists. Molecular modeling, further structure–activity relationship studies, and identification of novel atypical antipsychotic agents. J. Med. Chem. 47, 143–157.

Campiani, G., Butini, S., Trotta, F., Gemma, S., Nacci, V., Fiorini, I., Fattorusso, C., Catalanotti, B., Cagnotto, A., Mereghetti, I., Mennini, T., Minetti, P., Di Cesare, M.A., Stasi, M.A., Di Serio, S., Ghirardi, O., Tinti, O., Carminati, P., 2005. Novel atypical antipsychotic agents: rational design, an efficient palladium-catalyzed route, and pharmacological studies. J. Med. Chem. 48, 1705–1708.

Capuano, B., Crosby, I.T., Fallon, G.D., Lloyd, E.J., Yuriev, E., Egan, S.J., 2003. 2-Methyl-4-(4-methylpiperazin-1-yl)-10H-thieno[2,3-*b*] [1,5]benzodiazepine methanol solvate monohydrate. Acta Crystallogr. Sect. E: Struct. Rep. Online 59, O1367–O1369.

Crupi, V., Majolino, D., Mondello, M.R., Migliardo, P., Venuti, V., 2002. FT-IR spectroscopy: a powerful tool in pharmacology. J. Pharm. Biomed. Anal. 29, 1149–1152.

Fevotte, G., Calas, J., Puel, F., Hoff, C., 2004. Applications of NIR spectroscopy to monitoring and analyzing the solid state during industrial crystallization processes. Int. J. Pharm. 273, 159–169.

Fini, G., 2004. Applications of Raman spectroscopy to pharmacy. J. Raman Spectrosc. 35, 335–337.

Fogarasi, G., Zhou, X., Taylor, P.W., Pulay, P., 1992. The calculation of ab initio molecular geometries: efficient optimization by natural internal coordinates and empirical correction by offset forces. J. Am. Chem. Soc. 114, 8191–8202.

Frisch, M.J., Trucks, G.W., Schlegel, H.B., Scuseria, G.E., Cheeseman, J.R., Montgomery Jr., Vreven, T., Burant, J.C., Millam, J.M., Iyengar, S.S., Tomasi, J., Mennucci, B., Cossi, M., Scalmani, G., Rega, N., Nakatsuji, H., Hada, M., Ehara, M., Toyota, K., Hasegawa, J., Ishida, M., Nakajima, T., Honda, Y., Kitao, O., Klene, M., Li, X., Knox, J.E., Hratchian, H.P., Cross, J.B., Adamo, C., Jaramillo, J., Gomperts, R., Stratmann, R.E., Austin, A.J., Cammi, R., Pomelli, C., Ochterski, J.W., Morokuma, K., Voth, G.A., Salvador, P., Nnenberg, J.J., Dapprich, S., Daniels, A.D., Strain, M.C., Malick, D.K., Rabuck, A.D., Raghavachari, K., Ortiz, J.V., Cui, Q., Baboul, A.G., Clifford, S., Stefanov, B.B., Liu, G., Liashenko, A., Piskorz, P., Martin, R.L., Fox, D.J., Keith, T., Al-Laham, M.A., Nanayakkara, A., Challacombe, M., Gill, M.W., Chen, W., Wong, M.W., Gonzalez, C., Pople, J.A., Gaussian 03, Revision C.02. 2003.

Fulton, B., Goa, K.L., 1997. Olanzapine—A review of its pharmacological properties and therapeutic efficacy in the management of schizophrenia and related psychoses. Drugs 53, 281–298.

Grunenberg, A., Henck, J.O., Siesler, H.W., 1996. Theoretical derivation and practical application of energy/temperature diagrams as an instrument in preformulation studies of polymorphic drug substances. Int. J. Pharm. 129, 147–158.

Kelleher, J.P., Centorrino, F., Albert, M.J., Baldessarini, R.J., 2002. Advances in atypical antipsychotics for the treatment of schizophrenia: new formulations and new agents. CNS Drugs 16, 249–261.

Lee, C.T., Yang, W.T., Parr, R.G., 1988. Development of the Colle-Salvetti correlation-energy formula into a functional of the electron-density. Phys. Rev. B 37, 785–789.

Masamura, M., 2001. The effect of basis set superposition error on the convergence of interaction energies. Theor. Chem. Acc. 106, 301–313.

Martin, J.M.L., Van Alsenoy, C., 1995. Gar2ped. University of Antwerp.

Parr, R.G., Yang, W., 1989. Density Functional Theory of Atoms and Molecules. Oxford University Press, New York.

Petersson, G.A., Allaham, M.A., 1991. A complete basis set model chemistry. 2. Open-shell systems and the total energies of the 1st-row atoms. J. Chem. Phys. 94, 6081–6090.

Petersson, G.A., Bennett, A., Tensfeldt, T.G., Allaham, M.A., Shirley, W.A., Mantzaris, J., 1988. A complete basis set model chemistry. 1. The total energies of closed-shell atoms and hydrides of the 1st-row elements. J. Chem. Phys. 89, 2193–2218.

Polla, G.I., Vega, D.R., Lanza, H., Tombari, D.G., Baggio, R., Ayala, A.P., Filho, J.M., Fernandez, D., Leyva, G., Dartayet, G., 2005. Thermal behaviour and stability in olanzapine. Int. J. Pharm. 301, 33–40.

Pulay, P., Fogarasi, G., Pang, F., Boggs, J.E., 1979. Systematic ab initio gradient calculation of molecular geometries, force constants, and dipole moment derivatives. J. Am. Chem. Soc. 101, 2550–2560.

Reutzel-Edens, S.M., Bush, J.K., Magee, P.A., Stephenson, G.A., Byrn, S.R., 2003. Anhydrates and hydrates of olanzapine: crystallization, solid-state characterization, and structural relationships. Cryst. Growth Design 3, 897–907.

Varsanyi, G., 1969. Vibrational Spectra of Benzene Derivatives. Academic Press, New York.

Vieta, E., Goikolea, J.M., 2005. Atypical antipsychotics: newer options for mania and maintenance therapy. Bipolar Disord. 7, 21–33.

Wawrzycka-Gorczyca, I., Koziol, A.E., Glice, M., Cybulski, J., 2004. Polymorphic form II of 2-methyl-4-(4-methyl-1-piperazinyl)-10H-thieno-[2,3-*b*] [1, 5]benzodiazepine. Acta Crystallogr. Sect. E: Struct. Rep. Online 60, O66–O68.

Wawrzycka-Gorczyca, I., Mazur, L., Koziol, A.E., 2004. 2-Methyl-4-(4-methyl-1-piperazinyl)-10H-thieno[2,3-*b*] [1,5]benzodiazepine methanol solvate. Acta Crystallogr. Sect. E: Struct. Rep. Online 60, O69–O71.

Worrel, J.A., Marken, P.A., Ruehter, V.L., Beckman, S.E., 2000. Atypical antipsychotic agents: a critical review. Am. J. Health-Syst. Pharm. 57, 238–258.

Zhurko, G.A., Zhurko, D.A., 2005. ChemCraft Tool for Treatment of the Chemical Data. Available from: http://www.chemcraftprog.com.